# Spectroscopic Investigation of the Europium(3+) Ion in a New $ZnY_4W_3O_{16}$ Matrix

by **Elżbieta Tomaszewicz***[a]), **Malgorzata Guzik**[b]), **Joanna Cybińska**[b]), and **Janina Legendziewicz***[b])

[a]) Department of Inorganic and Analytical Chemistry, West Pomeranian University of Technology, Al. Piastów 42, PL-71-065 Szczecin (e-mail: tomela@ps.pl)

[b]) Faculty of Chemistry, University of Wrocław, Joliot-Curie 14, PL-50-383 Wrocław (e-mail: jl@wchuwr.pl)

Dedicated to Professor *Jean-Claude Bünzli* on the occasion of his 65th birthday.

A new Zn and Eu tungstate was characterized by spectroscopic techniques. This tungstate, of the formula $ZnEu_4W_3O_{16}$, crystallized in the orthorhombic system and was synthesized by a solid-state reaction. It melts incongruently at 1330°. The luminescent properties, including excitation and emission processes, luminescent dynamics, and local environments of the $Eu^{3+}$ ions in $ZnEu_4W_3O_{16}$ and $ZnY_4W_3O_{16}:Eu^{3+}$ diluted phases (1, 5, and 10 mol-% of $Eu^{3+}$ ion) were studied basing on the $f^6$-intraconfigurational transitions in the 250–720 nm spectral range. The excitation spectra of this system ($\lambda_{em}$ 615 and 470 nm) show broad bands with maxima at 265 and 315 nm related to the ligand-to-metal charge-transfer (LMCT) states. The emission spectra under excitation at the O → W (265 nm) and O → $Eu^{3+}$ (315 nm) LMCT states present the blue-green emission bands. The emission of tungstate groups mainly originate from the charge-transfer state of excited 2p orbitals of $O^{2-}$ to the empty orbitals of the central $W^{6+}$ ions. On the other hand, in the emission of the $Eu^{3+}$ ions, both the charge transfer from $O^{2-}$ to $Eu^{3+}$ and the energy transfer from $W^{6+}$ ions to $Eu^{3+}$ are involved. The emission spectra under excitation at the $^7F_0 \rightarrow {}^5L_6$ transition of the $Eu^{3+}$ ion (394 nm) of $ZnY_4W_3O_{16}:Eu^{3+}$ diluted samples show narrow emission lines from the $^5D_3$, $^5D_2$, and $^5D_1$ emitting states. The effect of the active-ion ($Eu^{3+}$) concentration on the colorimetric characteristic of the emissions of the compound under investigation are presented.

**Introduction.** – Due to the rapid rises of new semiconductor solid-state lighting devices – white-light-emitting diodes (WLEDs) – since the end of the last century, tremendous achievements have been made in the development of key materials and technology including semiconductor photoelectron, lighting project, and new luminescent materials. It is well known that tungstates belong to a very important family of inorganic materials used in the optical field due to their promising applications. The most investigated groups are $CaWO_4$ and $MgWO_4$ (as phosphors), as well as $ZnWO_4$, $CdWO_4$, and $PbWO_4$ (as scintillators) [1–3]. In the mentioned compounds, the efficient blue-green emission is intrinsic luminescent from the $WO_4$ tetrahedra (the scheelite family: $CaWO_4$ and $PbWO_4$) and from $WO_6$ octahedra (the wolframite family: $MgWO_4$, $ZnWO_4$, and $CdWO_4$). The optical properties of tungstates are mainly determined by charge-transfer (CT) transitions between the oxygen ($O^{2-}$) and tungsten ($W^{6+}$) ions within the tungstate molecular complexes. Moreover, they may also effectively transfer energy to rare-earth ions ($Eu^{3+}$) generating red emission, thus becoming potential white-light phosphors. One of the approaches to obtain white light is to combine a UV LED/laser diode with blue, green, and red (BGR) phosphors [4]. Therefore, the search for stable inorganic red phosphors containing rare-earth ions with high absorption in the near-UV/blue spectral region is a challenging task. $CaWO_4$ was first used as luminescent material in 1896, and due to a possibility of self-activation, it became a high-efficiency material emitting blue light under X-ray, electron-beam, and UV irradiation. First investigations on the rare-earth-activated tungstates were reported in the sixties by *Blasse* and *Bril* [5], and *Borchardt* [6]. Crystals of potassium lanthanide double tungstates and molybdates were reported by *Kaminskii* to be efficient luminescent hosts for rare-earth and transition-metal ions [7]. The phonon properties of $KEu(MO_4)_2$ (M = Mo, W) were described by *Macalik* [8]. Very extensive studies of the optical properties of double rare-earth molybdates and tungstates of the composition $M\mathit{RE}(XO_4)_2$ (M = Cs, K, Rb; *RE* = rare earth; X = Mo, W) were also reported [9]. The clustering process and the role of chain formation in lanthanide tungstates and molybdates on the optical behavior, mainly on radiative-transition probabilities and nonradiative phenomena, as well as the electron – lattice interactions in these matrices have been also investigated by us [10]. Promising luminescence properties of $Eu_2(WO_4)_3$ were well investigated by *Kodaira et al.* [1].

In recent years, great interest has been focused on lanthanide complexes with para- or diamagnetic transition-metal ions. The introduced d-electron metal ions play an important role in modulating magnetic and spectroscopic behaviors. The phosphors containing d- as well as f-electron metal ions have been less investigated [11][12]. The solid-state reaction is mostly used to prepare tungstates. Lately, it was reported that $ZnWO_4$ reacts with some rare-earth-metal tungstates ($\mathit{RE}_2WO_6$) to give the family of isostructural compounds with the general formula $Zn\mathit{RE}_4W_3O_{16}$ (*RE* = Y, Nd, Sm, Eu, Gd, Dy, and Ho) [13].

We now undertook spectral studies of the tungstate $ZnEu_4W_3O_{16}$ with the aim to understand its luminescence properties like electronic-transition probabilities, site symmetry, and energy-transfer processes. The tungstates doped with $Eu^{3+}$ ions, *i.e.*, $ZnY_{4-x}Eu_xW_3O_{16}$ (see *Sect. 2*), were also explored because the $Eu^{3+}$ ion may act as a common activator to detect local environment due to the super-sensitive f-f transitions. This activator can give very precious information about the site symmetry of the substituted ion. We studied the optical behavior of pure $ZnEu_4W_3O_{16}$ and of its yttrium-diluted analogues to determine the influence of the concentration of the doping $Eu^{3+}$ ion on the luminescence properties in the matrix, as far as it has not been reported yet in the literature.

**2. Experimental.** – 2.1. *Preparation of $ZnEu_4W_3O_{16}$ and $ZnY_{4-x}Eu_xW_3O_{16}$ Phases.* The starting materials were $ZnWO_4$, $Eu_2WO_6$, $Gd_2WO_6$, and $Y_2WO_6$. Zn and rare-earth-metal tungstates $Zn\mathit{RE}_4W_3O_{16}$, (*RE* = Y, Eu, Gd), *i.e.*, tungsten yttrium zinc oxide ($W_3Y_4ZnO_{16}$), europium tungsten zinc oxide ($Eu_4W_3ZnO_{16}$), and gadolinium tungsten zinc oxide ($Gd_4W_3ZnO_{16}$), were prepared by the solid-state-reaction route described previously [13]. The yttrium-diluted samples of the formula $ZnY_{4-x}Eu_xW_3O_{16}$ (denoted in the following as $ZnY_4W_3O_{16}:Eu^{3+}$), with the $Eu^{3+}$ concentrations 1, 5, and 10 mol-%, were synthesized by mixing $ZnWO_4$, $Eu_2WO_6$, and $Y_2WO_6$ in a suitable molar ratio and then heating under the same conditions as for the preparation of $Zn\mathit{RE}_4W_3O_{16}$ compounds. The X-ray powder diffraction, thermal analysis data, as well as the absorption, emission, and IR data established the composition and phase purity of the expected compounds and solid solns.

2.2. *Measurements.* XRD Phase analysis: *DRON*-3 diffractometer and $CoK_\alpha$ radiation ($\lambda$ 0.179021 nm); powder diffraction patterns were collected at r.t., and within the $2\theta$ range of 12 – 60°, at a stepped scan rate of 0.02° per step, and a count time of 1 s per step; for an indexing procedure, powder diffraction patterns were collected with a *X'Pert-PRO-Philips* diffractometer at the stepped scan rate of 0.02° per step and a count time of 10 s per step. IR Spectra: spectral range 300–1100 $cm^{-1}$; *Specord-M-80* spectrometer (*Carl Zeiss Jena*); powdered samples in KBr pellets. Emission Spectra: *SpectraPro-750* monochromator, equipped with a *Hamamatsu R928* photomultiplier and 1200 l/mm grating blazed at 500 nm; excitation source, 450 W xenon arc lamp coupled with a 275 mm excitation monochromator which used a 1800 l/mm grating blazed at 250 nm; excitation spectra were corrected for the excitation light intensity, while emission spectra were not corrected for the instrument response; measurements at room temperature and 77 K. Decay kinetics of luminescence: *F900* spectrometer from *Edinburgh Instruments.*

**3. Results and Discussion.** – 3.1. *Structural Considerations* (from XRD and IR data). On the basis of earlier studies concerning reactivity in the solid state between $ZnWO_4$ and some rare-earth-metal tungstates $RE_2WO_6$ ($RE$ = Y, Nd, Sm, Eu, Gd, Dy, and Ho), it was ascertained that these compounds are not mutually inert in air and react to give the family of new compounds with the formula $ZnRE_4W_3O_{16}$ [13]. These phases were synthesized by means of a conventional ceramic method according to the reaction $ZnWO_{4(s)} + 2RE_2WO_{6(s)} = ZnRE_4W_3O_{16(s)}$ [13].

The $Zn(RE)_4W_3O_{16}$ melt incongruently or decompose in the solid state above 1250° [13]. Powder diffraction patterns of the $ZnRE_4W_3O_{16}$ were subjected to indexing performed by means of the POWDER [14] and DICVOL [15] programs. Very convergent solutions were obtained by the indexing procedure with these programs [13]. The $ZnRE_4W_3O_{16}$ phase crystallizes in the orthorhombic system with the following lattice constants for the lanthanides $RE$ = Ho to Nd: $a$ = 17.4110(1) to 17.8237(2), $b$ = 7.2716(0) to 7.4565(3), and $c$ = 7.2185(2) to 7.3495(7) Å [13]. The $ZnY_4W_3O_{16}$ compound has the following parameters of the unit cell: $a$ = 17.4241(0), $b$ = 7.2828(2), and $c$ = 7.1852(0) Å [13]. The unit cell of each $ZnRE_4W_3O_{16}$ is primitive and contains three molecules of the compound ($Z$ = 3) – a very seldom met number of molecules per unit for the orthorhombic system [12]. The lattice parameters and cell volumes of the $ZnRE_4W_3O_{16}$ decrease with decreasing radius of the rare-earth ion. The $ZnRE_4W_3O_{16}$ are isostructural and can form substitutional solid solutions. *Fig. 1* presents the powder diffraction patterns of the starting materials $ZnWO_4$, $Eu_2WO_6$, and $Y_2WO_6$), of one compound of the $ZnRE_4W_3O_{16}$ family, *i.e.*, $ZnEu_4W_3O_{16}$, and of the solid solution of 1 mol-% of $ZnEu_4W_3O_{16}$ in $ZnY_4W_3O_{16}$ ($ZnY_4W_3O_{16}$ : $Eu^{3+}$ 1%). After indexing the $ZnRE_4W_3O_{16}$ powder diffraction patterns, one can conclude that these compounds are not isostructural with the already known cadmium and rare-earth-metal molybdates with an analogous type of the chemical formula, $CdRE_4Mo_3O_{16}$ [16]. The next family of compounds, with a type structure identical to that of the $ZnRE_4W_3O_{16}$ family and the analogous chemical formula $CoRE_4W_3O_{16}$, was obtained by the solid-state reaction of $CoWO_4$ with $RE_2WO_6$ only for $RE$ = Sm, Eu, and Gd [17].

*Fig. 2* shows the IR spectra of $ZnGd_4W_3O_{16}$ as well as of $CoGd_4W_3O_{16}$. On the basis of literature information [18] concerning the IR data of binary and ternary lanthanide tungstates with various types of isolated and joint tungsten polyhedra, it was found that absorption bands with maxima at 874 $cm^{-1}$ ($ZnGd_4W_3O_{16}$) or 872 $cm^{-1}$ ($CoGd_4W_3O_{16}$) (*Fig. 2*) can be assigned to the symmetric stretching vibrations of short terminal W–O bonds. This fact indicates the presence, in structures of the type $MRE_4W_3O_{16}$ (M =

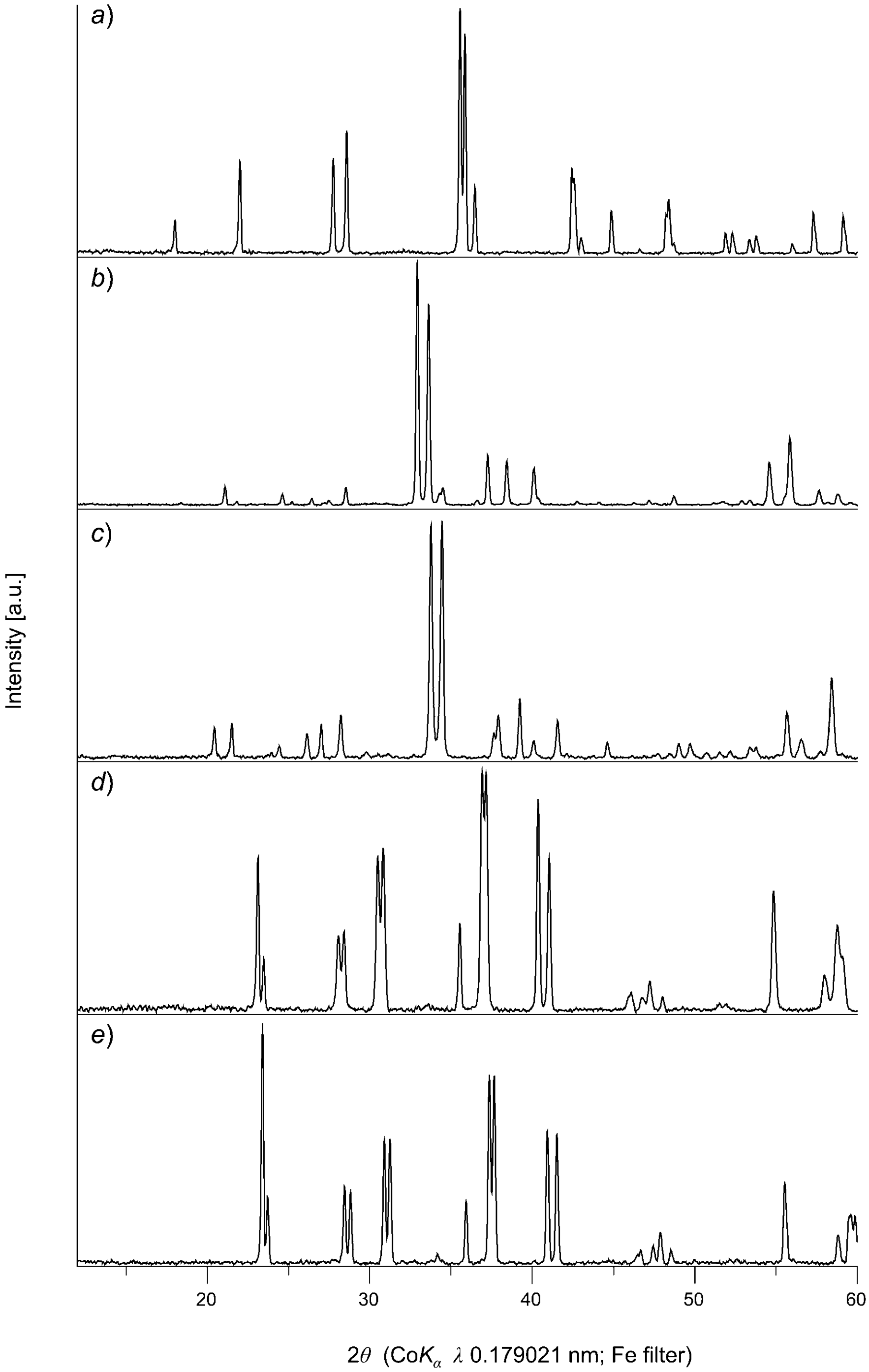


Fig. 1. *Powder diffraction patterns of* a) $ZnWO_4$, b) $Eu_2WO_6$, c) $Y_2WO_6$, d) $ZnEu_4W_3O_{16}$, *and* e) *solid solution* $ZnY_{3.99}Eu_{0.01}W_3O_{16}$

Co, Zn), the following structural elements: trihedral bipyramid $WO_5$ or $WO_6$ octahedra joint by O-bridges forming $[(W_2O_9)^{6-}]\infty$ chains [18]. The trihedral bipyramids $WO_5$ were found in structures of the $RE_2WO_6$ phases (stretching vibrations of short terminal W–O bonds in the region of 880–870 $cm^{-1}$) [18]. In turn, the structural element $[(W_2O_9)^{6-}]\infty$ was found in structures of the $RE_2W_2O_9$ family ($RE$ = Pr, Nd, Sm to Gd) (stretching vibrations of short terminal W–O bonds in the region of 885–867 $cm^{-1}$) [18].

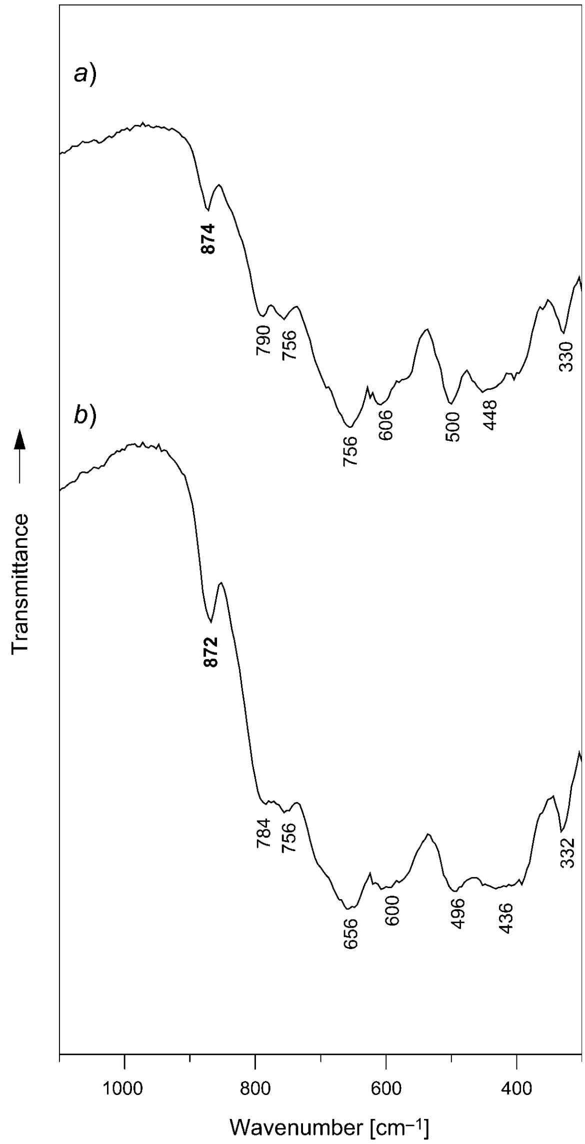


Fig. 2. *IR Spectra of* a) *$ZnGd_4W_3O_{16}$ and* b) *$CoGd_4W_3O_{16}$*

The thermal properties of the M$RE_4W_3O_{16}$ (incongruent melting or decomposition in the solid state) caused that our effort to obtain these compounds as single crystals was not successful. X-Ray diffraction with *Rietveld*-refinement simulation will be performed in a near future. This procedure will allow to obtain details concerning the structure of the tungstates under investigations.

3.2. *Photoluminescent Study.* The UV/VIS diffuse reflectance spectra of powdered samples of $ZnGd_4W_3O_{16}$, $ZnEu_4W_3O_{16}$, and the $ZnY_4W_3O_{16}:Eu^{3+}$ 1% phase in the region from 200 to 700 nm are shown in *Fig. 3*. The $ZnGd_4W_3O_{16}$ compound presents high-intensity broad bands in the UV region assigned to a CT transition from $O^{2-}$ 2p orbitals to the empty $W^{6+}$ 5d orbitals. The doped $ZnY_4W_3O_{16}:Eu^{3+}$ 1% presents similar absorption bands to those of $ZnGd_4W_3O_{16}$ but an additional component at around 315 nm can be observed. This band could arise from the O $\rightarrow$ $Eu^{3+}$ CT transition. Thus, UV radiation is efficiently absorbed by the CT state of $Eu^{3+}-O^{2-}$. According to the literature, location of the CT bands for $ZnWO_4$ or $Eu_2(WO_4)_3$ are around 250–265 and 315 nm [1][11], but in most reports, the contributions of these two components cannot be distinguished due to spectral overlapping.

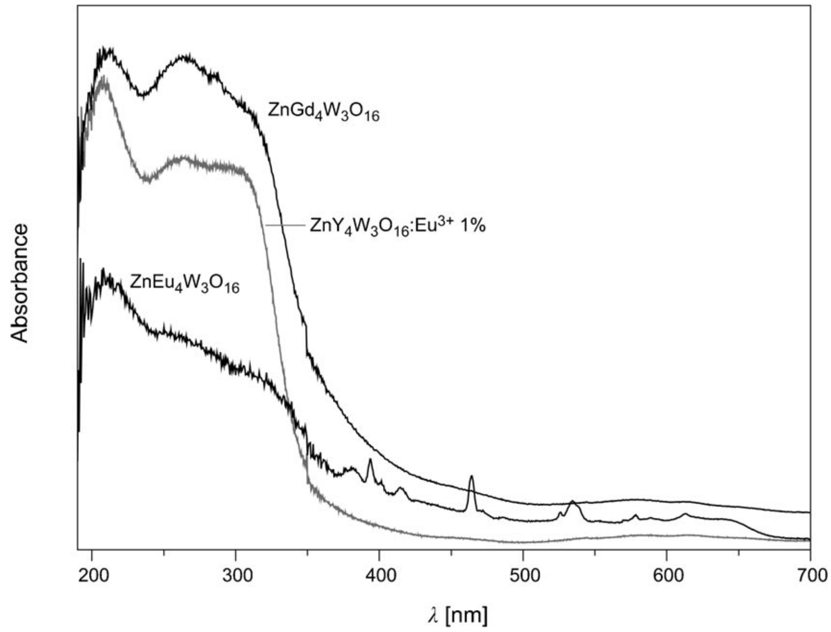


Fig. 3. *Diffuse reflectance spectra of powdered samples of $ZnGd_4W_3O_{16}$, $ZnEu_4W_3O_{16}$, and $ZnY_4W_3O_{16}:Eu^{3+}$ 1% at room temperature*

It is not surprising that the $Eu^{3+}$ 4f-4f transitions (spin-forbidden) are weak in comparison to the CT bands. *Fig. 4* presents the absorption spectrum of $ZnEu_4W_3O_{16}$ in the 375–700 nm range recorded at room temperature. The narrow absorption lines characteristic of the $4f^6$-intraconfigurational transition originate from the $Eu^{3+}$ ion. Their low intensity arises from the fact that they are forbidden by the *Laporte* rule, while transitions from LMCT state are electronically allowed. The absorption spectra consist of a large number of lines assigned to $^7F_0 \rightarrow {}^5D_J$ ($J = 0-3$), $^5L_J$, $^5G_J$ transitions. At room temperature, one can also observe transitions from the thermally populated $^7F_1$ and $^7F_2$ states, thus recorded bands correspond to $^7F_{J(1,\ 2)} \rightarrow {}^5D_J$. The $^7F_0 \rightarrow {}^5D_0$ transition is a single line.

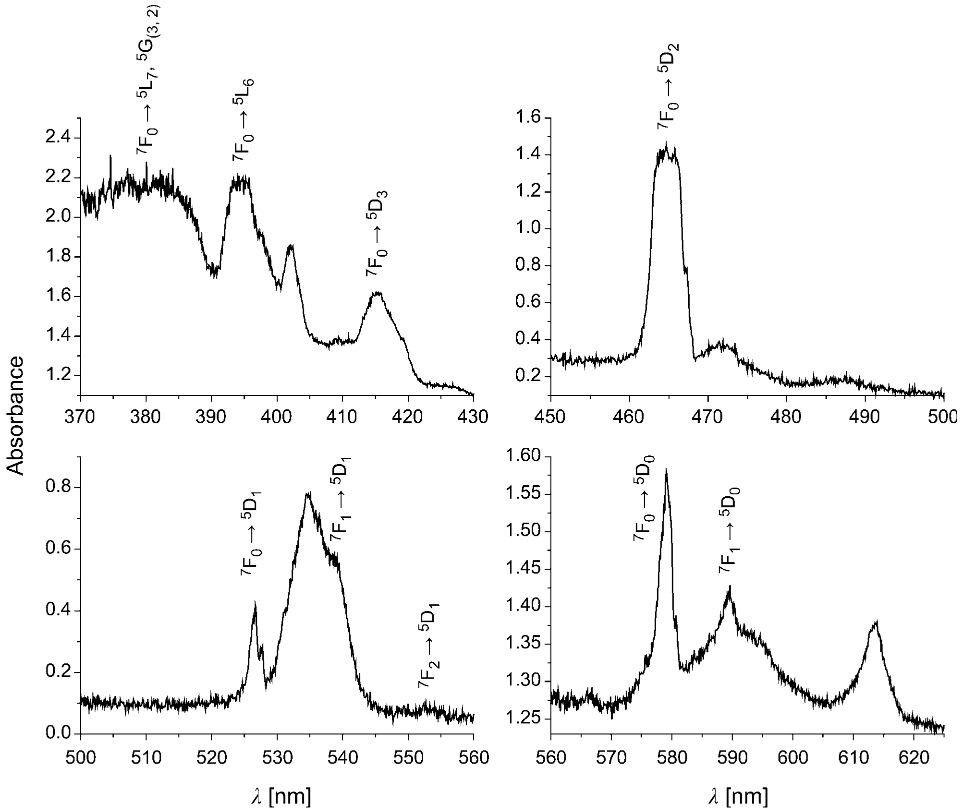


Fig. 4. *Absorption spectrum at room temperature of $ZnEu_4W_3O_{16}$ corresponding to the $^7F_0 \rightarrow {}^5L_{6,7}$, $^5G_{(3,2)}$, and $^7F_0 \rightarrow {}^5D_{0-3}$ transitions*

3.2.1. *Excitation Spectra.* The excitation spectra of the $ZnY_4W_3O_{16}$:$Eu^{3+}$ 10%, presented in *Fig. 5*, were measured at room and liquid-$N_2$ temperature, under detection at λ 615 nm. The broad band observed in the range 250–320 nm corresponds to the LMCT states from the O → W and O → $Eu^{3+}$ transitions at *ca.* 265 and 310 nm, respectively. The LMCT bands contain sharp lines at 303 and 320 nm, corresponding to the $^7F_0 \rightarrow {}^5F_{2,4}$ and $^5H_3$ transitions of the $Eu^{3+}$ ion. In the spectral region of 350–600 nm, one can find many sharp lines corresponding to the $^7F_0 \rightarrow {}^5D_J$ ($J = 0-3$) transitions of the $Eu^{3+}$ ion. Analysis of the low-temperature excitation spectrum indicates that some of these lines could be accompanied by a number of satellites of vibronic or ion-pair origin as it was observed in the case of potassium europium double tungstates [10]. In the spectra recorded at room temperature, transitions originating from $^7F_{1,2}$ to different $^5D_J$ states are also present (see *Figs. 4* and *5*). In this region, the thermal population of $^7F_{1,2}$ is responsible for the complex shape of the spectra. IR Data suggest the presence of trihedral $WO_5$ bipyramids or joint $WO_6$ octahedra forming chains $[(W_2O_9)^{6-}]\infty$ by O-bridges. Formation of the polymeric structure could be confirmed by additional lines which have a vibronic origin. In the excitation spectra of $ZnY_4W_3O_{16}:Eu^{3+}$ 10% the weak sidebands accompanying the $^7F_0 \rightarrow {}^5D_0$ and $^7F_0 \rightarrow {}^5D_2$ transitions are due to vibronic coupling (see *Fig. 5*). The vibronic structure was more pronounced for the concentrated sample $ZnEu_4W_3O_{16}$. These lines could correspond to the O-bridge-bond vibrations. However, their intensities are very low. *Fig. 6* shows the excitation spectra of the $Eu^{3+}$ emission at 470 nm of the $ZnY_4W_3O_{16}:Eu^{3+}$ 10% phase recorded at room and low temperature. They present the band assigned to the CT transition of $WO_6$ and Eu–O, which corresponds well to the results obtained from the reflectance spectra (*Fig. 3*). The overlap of excitation spectra of tungstate groups and $Eu^{3+}$ ions was also observed previously for $ZnWO_4:Eu^{3+}$ [11]. These spectra consist also of sharp lines due to transitions within the $4f^6$ shell of the $Eu^{3+}$ ion. In the excitation and emission spectra, the vibronic components associated with the $Eu^{3+}$ ion were observed as discussed above. They reflect electron-lattice interactions, which also affect the nonradiative transitions [10].

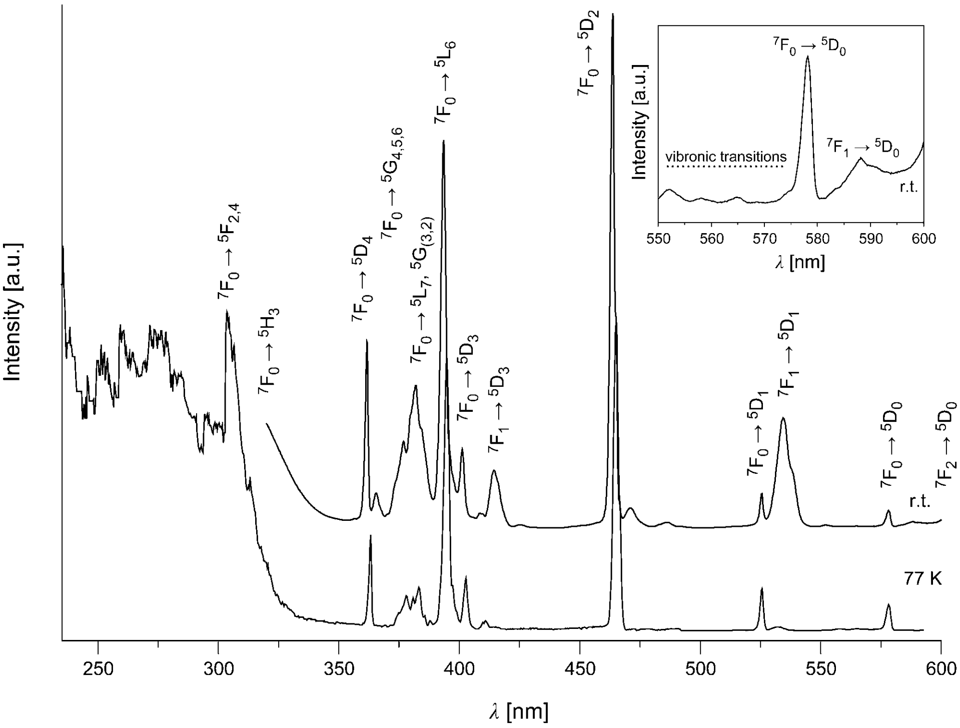


Fig. 5. *Excitation spectra of the $ZnY_4W_3O_{16}:Eu^{3+}$ 10% with emission monitored at 615 nm at room and liquid-$N_2$ temperature*

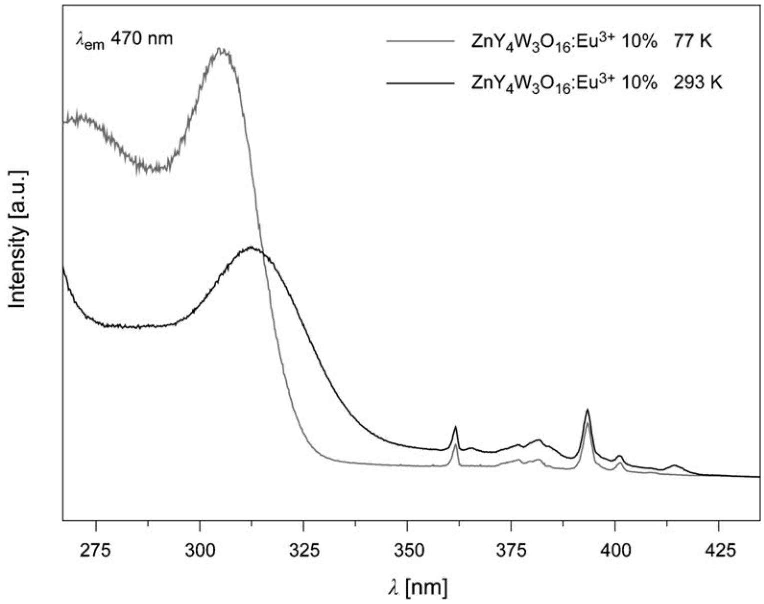


Fig. 6. *Excitation spectra of the $ZnY_4W_3O_{16}:Eu^{3+}$ 10% sample with emission monitored at 490 nm at room and liquid $N_2$-temperature*

3.2.2. *Emission Spectra.* The emission spectra of the $ZnY_4W_3O_{16}:Eu^{3+}$ 10% phase in the range from 380 to 735 nm recorded at room and low temperature are shown in *Fig. 7.* Under excitation at 315 nm (Xe lamp), the spectrum exhibits a blue broad band emission in the 400–575 nm region with the maximum at *ca.* 490 nm. According to the IR-absorption results, the $WO_6$ octahedral structure are the luminescent centers, and a CT transition between the $O^{2-}$ 2p orbital and empty d orbitals of the central $W^{6+}$ ion takes place. Excitation into the tungstate groups not only gives the typical emission centered at 490–500 nm but also yields the characteristic emissions of the $Eu^{3+}$ ion, the transitions from the excited $^5D_0$ to ground $^7F_J$ states. The emission spectra recorded at room and liquid-$N_2$ temperature with excitation at the $O \rightarrow W$ and $O \rightarrow Eu^{3+}$ LMCT transitions at *ca.* 265 nm (not presented here) and 315 nm, respectively, do not contain emission bands from the $^5D_3$ and $^5D_2$ states, while they appear under direct excitation into the $^5L_6$ level of the $Eu^{3+}$ ion (*Fig. 7*). According to *Fonger* and *Struck* [19], this phenomenon occurs due to a resonance crossover between the $O \rightarrow W$ and $O \rightarrow Eu^{3+}$ LMCT states and $^5D_J$ emitting levels ($J = 3$, 2, and 1) near the LMCT-band maximum considering that the low-laying LMCT state skips the higher lying $^5D_J$ emitting levels during its relaxation process [20]. Similar results were obtained by *Brito* and co-workers for $Eu_2(WO_4)_3$ [1]. Upon CT excitation ($O \rightarrow W$ LMCT states at 260 nm), they observed only transition from the emitting $^5D_1$ level. This was explained by feeding of the $O \rightarrow W$ and $O \rightarrow Eu^{3+}$ LMCT states upon excitation into the 4f states, which shifts the $^5D_J$ ($J = 3$, 2, and 1) population to the lower $^5D_0$ emitting level and leads to a luminescence quenching in the following order $^5D_3 > {}^5D_2 > {}^5D_1 > {}^5D_0$ with increasing temperature [1] [19]. For the compounds under investigation, the components from $^5D_1$

were observed both at room and low temperatures. The profile of the emission spectra under 265 nm excitation (not presented here) is the same as in the case of excitation at 315 nm. When increasing the doping level of the $Eu^{3+}$ ions in the $ZnY_4W_3O_{16}$ matrix, gradual diminishing of the emission of $WO_6$ due to the efficient energy transfer from $WO_6$ to the $Eu^{3+}$ ion is observed. The CT-excitation band of $Eu^{3+}$ and the emission band of $WO_6$ are partially overlapping each other. *Fig. 8* presents the emission spectra of $ZnY_4W_3O_{16}:Eu^{3+}$ with different $Eu^{3+}$-ion-doping levels, recorded at room temperature under excitation at $\lambda_{ex}$ 315 nm.

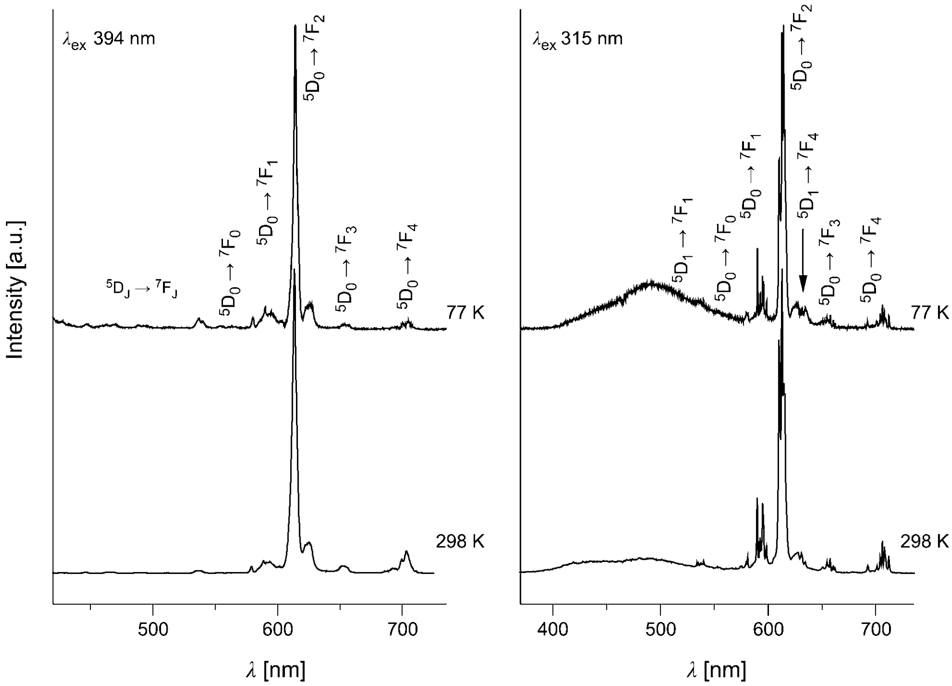


Fig. 7. *Emission spectra of $ZnY_4W_3O_{16}:Eu^{3+}$ 10% at room temperature and 77 K, $\lambda_{ex}$ 315 and 394 nm*

Under direct excitation into the band corresponding to the $^7F_0 \rightarrow {}^5L_6$ transition of the $Eu^{3+}$ ion ($\lambda_{ex}$ 394 nm), the sample $ZnY_4W_3O_{16}:Eu^{3+}$ 10% emitted red light with a number of narrow lines due to the 4f–4f ($^5D_0 \rightarrow {}^7F_J$) transitions. The emission bands arising from $^5D_J$ emitting levels ($J = 3$, 2, and 1) were also observed. At low temperature, their resolution is higher than at room temperature (see *Fig. 9*). The profiles of fluorescence spectra of phosphors doped with $Eu^{3+}$ ions show that among all emission transitions from higher-localized excited states, the most intensive is that corresponding to the $^5D_1 \rightarrow {}^7F_1$ ones at 538 nm. The presence of a strongly forbidden $^5D_0 \rightarrow {}^7F_0$ transition at *ca.* 580 nm and the high-intensity hypersensitive $^5D_0 \rightarrow {}^7F_2$ electric-dipole transition at 615 nm indicates that the $Eu^{3+}$ ions exist in an environment with low symmetry. The electric-dipole transition is allowed only under the condition

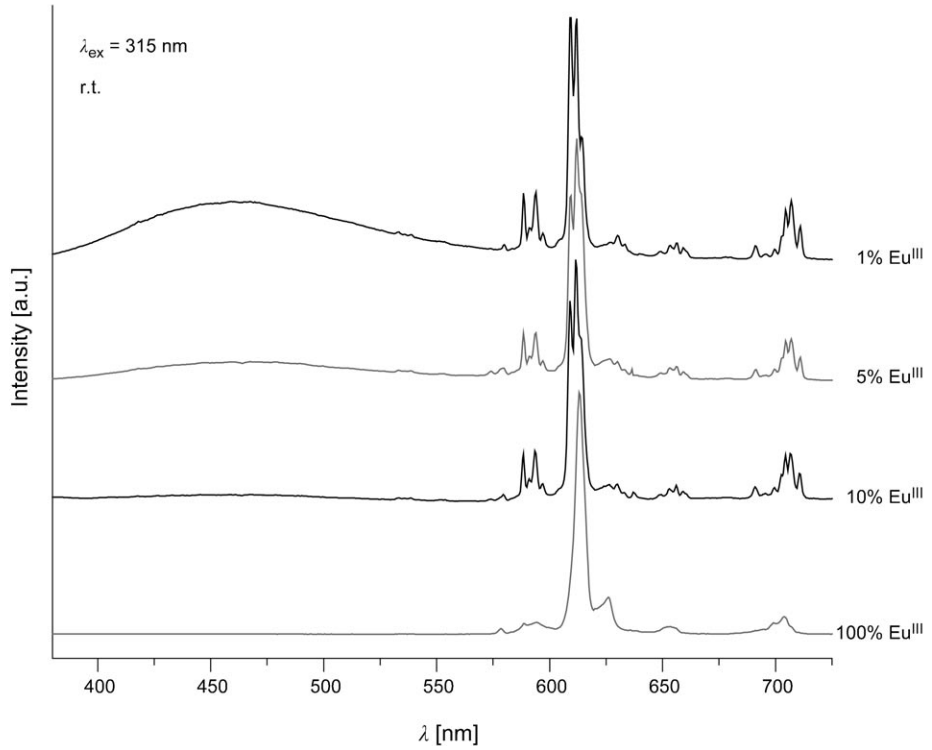


Fig. 8. *Emission spectra of $ZnY_4W_3O_{16}:Eu^{3+}$ and $ZnEu_4W_3O_{16}$* (100% $Eu^{3+}$) *at room temperature and $\lambda_{ex}$ 315 nm*

that the $Eu^{3+}$ ion occupies a site without an inversion center and is sensitive to local symmetry. The presence of the $^5D_0 \rightarrow {}^7F_0$ transition indicates that the $Eu^{3+}$ ions could be located in one of the $C_{nv}$, $C_n$, or $C_s$ symmetry groups. The large ratio of the fluorescence intensities of the $^5D_0 \rightarrow {}^7F_2/{}^5D_0 \rightarrow {}^7F_1$ transitions implies a low symmetry field at the $Eu^{3+}$ site. The $ZnY_4W_3O_{16}:Eu^{3+}$ is an example of a sample in which the $Eu^{3+}$ ions occupy lattice sites with no center of symmetry. Other emission lines are located at 583–601 ($^5D_0 \rightarrow {}^7F_1$), 604–642 ($^5D_0 \rightarrow {}^7F_2$), 646–666 ($^5D_0 \rightarrow {}^7F_3$), and 690–723 ($^5D_0 \rightarrow {}^7F_4$) nm. The $Eu^{3+}$ emission peaks are dominated by a peak at 612 ($^5D_0 \rightarrow {}^7F_2$) nm. Under 394 nm excitation both at room and liquid-$N_2$ temperature, only one component is observed for the $^5D_0 \rightarrow {}^7F_0$ transition confirming emission from only one site of $Eu^{3+}$. One can observe also a low number of the components in all other transitions. For the concentrated sample $ZnEu_4W_3O_{16}$, only fluorescence from the $^5D_0$ level to levels of the $^7F$ ground multiplet is observed. No fluorescence from $^5D_1$ or higher excited states of $Eu^{3+}$ is present, what is not unexpected since at high $Eu^{3+}$ concentrations, these states are usually quenched by cross-relaxation, and ion–ion interactions become more effective; thus $^5D_0$ is the only metastable state. The decay curve for the $^5D_0$ level ($^5D_0 \rightarrow {}^7F_2$ transition) could be well fitted with a single exponential function and, in agreement with the observation of a single $^5D_0 \rightarrow {}^7F_0$

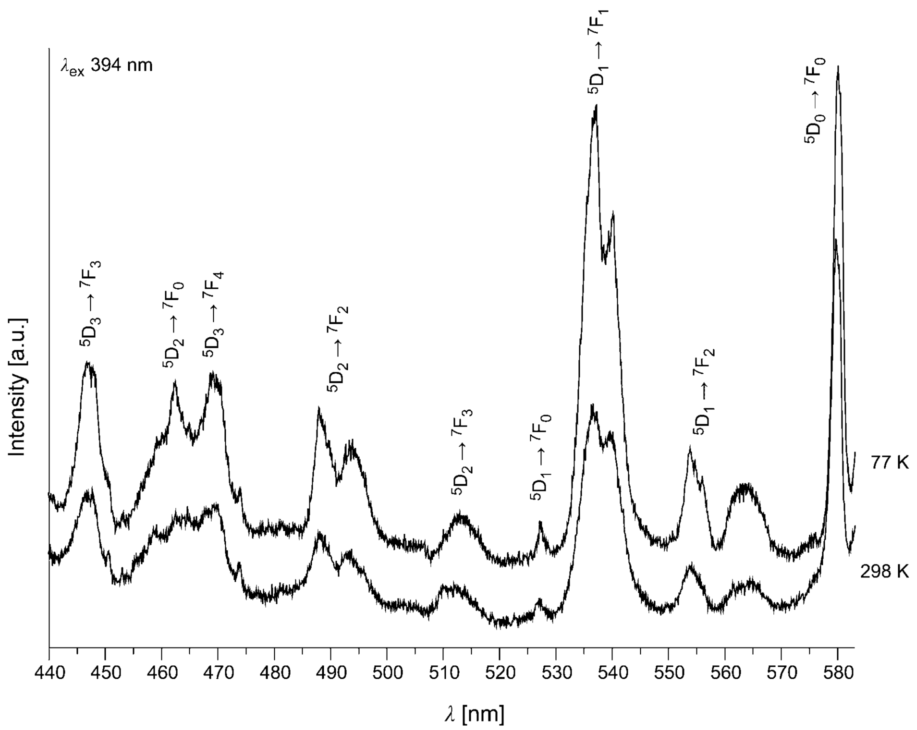


Fig. 9. *Emission spectra of* $ZnY_4W_3O_{16}:Eu^{3+}$ *10% at room temperature and 77 K and* $\lambda_{ex}$ *394 nm*

transition. This can indicate also that only the site of one $Eu^{3+}$ is the emitting center in the tungstates. The decay-time curves for the studied samples were measured at room and liquid-$N_2$ temperature. The compounds were excited with $\lambda_{ex}$ 355 nm of a Nd : YAG laser and observed at 615 nm. The decay times for $ZnY_4W_3O_{16}:Eu^{3+}$ 5%, $ZnY_4W_3O_{16}:Eu^{3+}$ 10%, and $ZnEu_4W_3O_{16}$ are collected in *Table 1*. This decay times were mainly monoexponential functions. This can suggest (for the systems with complex $^5D_0-{}^7F_0$ range) a fast energy transfer from one site to another one. Emission lifetimes of $Eu^{3+}$ for the fully concentrated sample $ZnEu_4W_3O_{16}$ are very short (0.05 ms). For this system, we observe a slight temperature dependence because a decrease of temperature leads to an increase of the decay time, but the latter is still short (0.14 ms at 77 K). For the diluted samples, the decay times are much longer – in

Table 1. *Emission Decay Times for* $ZnY_4W_3O_{16}:Eu^{3+}$ *5%,* $ZnY_4W_3O_{16}:Eu^{3+}$ *10%, and* $ZnEu_4W_3O_{16}$

| | $\lambda_{ex}$ [nm] | $\lambda_{obs}$ [nm] | Emission decay time [ms] | |
|---|---|---|---|---|
| | | | room temp. | 77 K |
| $ZnEu_4W_3O_{16}$ | 355 | 615 | 0.05 | 0.14 |
| $ZnY_4W_3O_{16}:Eu^{3+}$ 5% | 355 | 615 | 0.29 | 0.36 |
| $ZnY_4W_3O_{16}:Eu^{3+}$ 10% | 355 | 615 | 0.30 | 0.35 |

the range of 0.3 ms what is comparable to the results presented earlier by *Macalik* and co-workers for double tungstates [9]. The decay times for 5 and 10% concentration samples are almost temperature independent.

The number of *Stark* components observed in the spectra recorded under 394 nm excitation and predicted on the basis of the selection rule for respective symmetries suggests the $C_{2v}$ symmetry of the $Eu^{3+}$ ion in the samples under investigation. The number of components in the emission spectra under 394 nm and the decay-time measurements may lead to the conclusion that the active ion $Eu^{3+}$ occupies only one symmetry site. However, the shape of the spectra and the number of components strongly depend on the excitation energy. *Fig. 10* presents the emission spectra of $ZnY_4W_3O_{16}:Eu^{3+}$ 10% at 77 K under 315 and 394 nm excitation. Upon excitation in the tungstate group ($\lambda_{ex}$ 315 nm), the bands corresponding to f-f transitions become more complex. The shape of the spectra and number of components in the spectra under both 315 nm and (not presented here) 265 nm excitation are the same and exceed those expected for a single metal center in the crystal. When changing the excitation energy (394 → 315 nm), a change of the fluorescence intensities of the $^5D_0 \rightarrow {}^7F_0$ transition was observed (see *Fig. 11*). Its decreasing and also the appearance of additional components at 573.8, 574.8, 578.8, and 580.2 nm in the range of the $^5D_0 \rightarrow {}^7F_0$ transition were observed in the spectra excited in the tungstate group ($\lambda_{ex}$ 315 nm), while upon $\lambda_{ex}$ 394 nm, one can observe only one line at 580.1 nm. The $^5D_0 \rightarrow {}^7F_0$ emission line

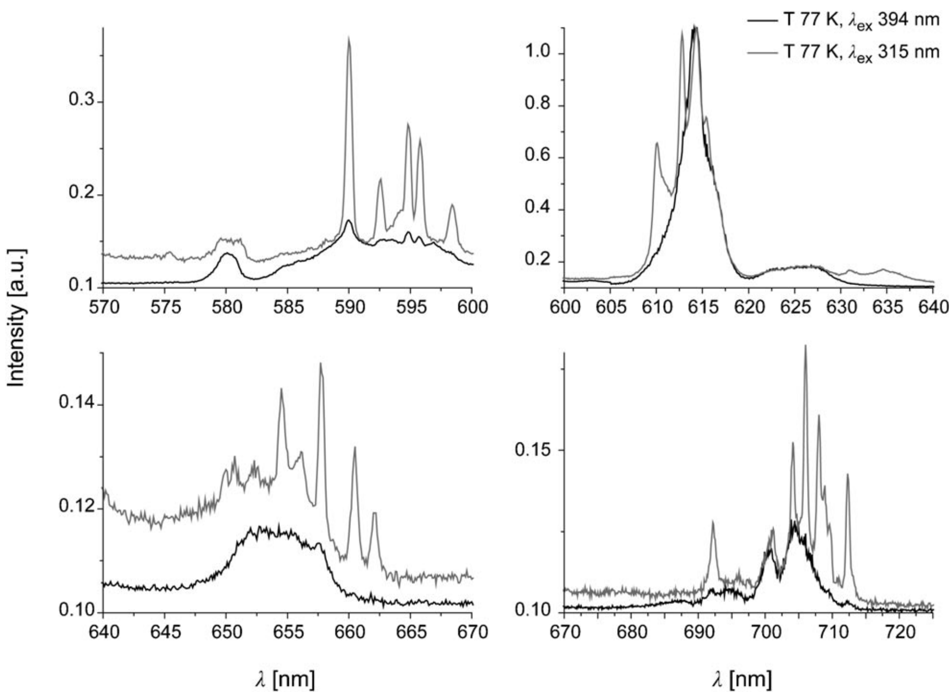


Fig. 10. *Emission spectra of $ZnY_4W_3O_{16}:Eu^{3+}$ 10% at liquid-$N_2$ temperature, $\lambda_{ex}$ 315 and 394 nm*

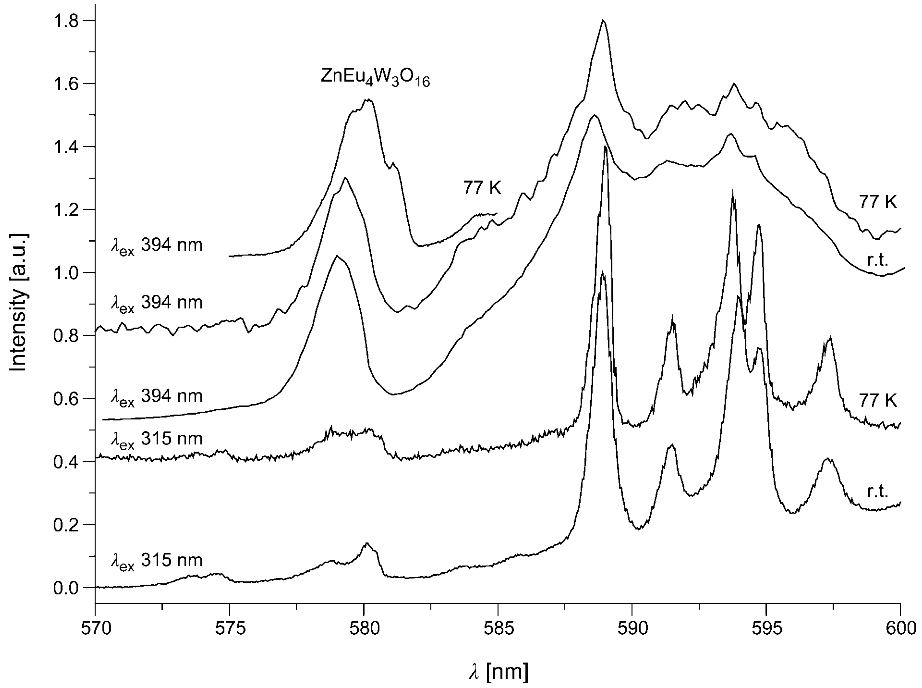


Fig. 11. *Emission* ($^5D_0 \rightarrow {}^7F_0$ and $^5D_0 \rightarrow {}^7F_1$ transitions) *spectra of* $ZnY_4W_3O_{16}$*:*$Eu^{3+}$ 10% *and* $ZnEu_4W_3O_{16}$ *at room and liquid-*$N_2$ *temperature and* $\lambda_{ex}$ *315 and 394 nm*

acquires special importance because it reveals the presence of crystallographically inequivalent sites in a host matrix. *Table 2* contains the transition energies of the $^5D_J \rightarrow {}^7F_J$ manifolds observed in the emission spectra of $ZnY_4W_3O_{16}:Eu^{3+}$ 10% at 77 K under 315 and 394 nm excitation. The bands corresponding to individual transitions in the emission spectra under 315 nm excitation are broad, and their width is similar to those recorded under 394 nm excitation. Additional components appearing in the spectra excited at 315 nm evidence the presence of more than one site occupied by the $Eu^{3+}$ ion in zinc tungstates. It is known that in tungstates and molybdates of rare-earth ions, lanthanides can create two or three different polyhedra with the O ions. For example, for $RE_2W_2O_9$, one can distinguish two nonequivalent *RE* ions, with a coordination $REO_7$ (monocapped trigonal prism) and $REO_8$ (bicapped trigonal prism). It can also be possible that, in spite of the fact that we have only octahedra, there are different bonding lengths, thus we see two different distorted octahedra.

The presented results are the first spectroscopic analysis of the new compound $ZnEu_4W_3O_{16}$ and of the $ZnY_4W_3O_{16}:Eu^{3+}$ diluted phases. Assignment of separated *Stark* components to the respective symmetry site will be possible by site-selective excitation of a particular site or level. The site-selective spectroscopy and refinement structure by using X-ray powder diffraction with the *Rietveld* methods would allow us to determine precisely the symmetry and number of sites occupied by the active ion in this new matrix. This will be the subject our future investigations.

Table 2. *Transition Energies of the* $^5D_J \rightarrow {}^7F_J$ *Manifolds* (in $cm^{-1}$) *Observed in the Emission Spectra of* $ZnY_4W_3O_{16}:Eu^{3+}$ *10% at 77 K*

| Transition | Energy [nm]–[$cm^{-1}$] | | Transition | Energy [nm]–[$cm^{-1}$] | |
|---|---|---|---|---|---|
| | $\lambda_{ex}$ 394 nm | $\lambda_{ex}$ 315 nm | | $\lambda_{ex}$ 394 nm | $\lambda_{ex}$ 315 nm |
| $^5D_3 \rightarrow {}^7F_3$ | 446.7–22386 | | $^5D_0 \rightarrow {}^7F_0$ | 580.1–17238 | 573.8–17428 |
| | 447.8–22331 | | | | 574.8–17397 |
| | 450.5–22197 | | | | 578.8–17277 |
| | | | | | 580.2–17235 |
| $^5D_3 \rightarrow {}^7F_0$ + | 460.0–21739 | | | | |
| $^5D_3 \rightarrow {}^7F_4$ | 462.4–21626 | | $^5D_0 \rightarrow {}^7F_1$ | 590.0–16949 | 590.0–16949 |
| | 464.8–21515 | | | 592.8–16869 | 592.6–16875 |
| | 468.6–21340 | | | 594.8–16812 | 594.8–16812 |
| | 470.5–21254 | | | 595.7–16787 | 595.8–16874 |
| | 474.0–21097 | | | 596.8–16756 | 598.4–16711 |
| | | | | 598.3–16714 | |
| $^5D_2 \rightarrow {}^7F_1$ | 479.0–20877 | | | | |
| | 481.3–20777 | | $^5D_0 \rightarrow {}^7F_2$ | 612.9–16316 | 610.1–16391 |
| | 483.6–20678 | | | 614.3–16279 | 612.8–16318 |
| | | | | | 614.3–16279 |
| $^5D_2 \rightarrow {}^7F_2$ | 487.9–20497 | | | | 615.4–16250 |
| | 489.6–20425 | | | | |
| | 493.9–20247 | | $^5D_0 \rightarrow {}^7F_3$ | 652.0–15337 | 650.0–15385 |
| | 495.8–20169 | | | 655.6–15253 | 650.7–15368 |
| | | | | 657.5–15209 | 652.3–15330 |
| $^5D_2 \rightarrow {}^7F_3$ | 510.0–19608 | | | | 654.5–15279 |
| | 512.9–19497 | | | | 656.1–15242 |
| | | | | | 657.7–15204 |
| $^5D_1 \rightarrow {}^7F_0$ | 527.1–18972 | | | | 660.5–15140 |
| | | | | | 662.0–15106 |
| $^5D_1 \rightarrow {}^7F_1$ | 537.2–18615 | 535.1–18688 | | | |
| | 540.1–18515 | 537.6–18601 | $^5D_0 \rightarrow {}^7F_4$ | 691.8–14455 | 692.2–14447 |
| | 541.6–18464 | 540.1–18515 | | 695.9–14370 | 696.1–14366 |
| | | | | 700.9–14267 | 697.4–14339 |
| $^5D_1 \rightarrow {}^7F_2$ | 553.8–18057 | | | 703.9–14207 | 701.2–14261 |
| | 556.0–17986 | | | 705.8–14168 | 704.1–14203 |
| | 564.2–17724 | | | 709.5–14094 | 706.0–14164 |
| | | | | 712.2–14041 | 708.0–14124 |
| | | | | | 708.9–14106 |
| | | | | | 709.6–14092 |
| | | | | | 711.0–14065 |
| | | | | | 712.3–14039 |

3.2.3. *Color Points and Colorimetric Characterization.* We analyzed also the ability of the materials as candidates for phosphor application. To characterize the luminescence ($\lambda_{ex}$ 315 nm) of the systems under investigation with respect to their emission color at 293 K, the *CIE* ($x$, $y$) coordinates were calculated [21]. A coordinate system ($x$, $y$) to characterize colors has been defined by the *Commission Internationale de l'Eclairage* (*CIE*) [22]. The location of the color coordinates of each phosphor in the *CIE* chromatic diagram is presented in *Fig. 12*. Taking into account the potential

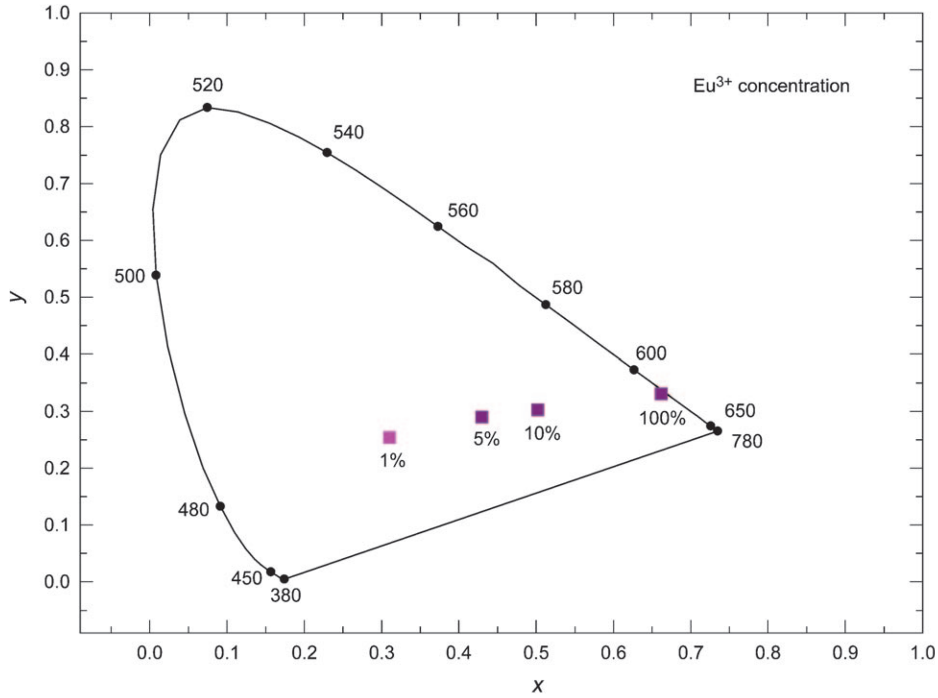


Fig. 12. CIE *Chromatic diagram showing the influence of the concentration of the* $Eu^{3+}$ *ion on the chromatic coordinates of the* $ZnY_4W_3O_{16}:Eu^{3+}$ *phases containing 1, 5, 10, and 100% of* $Eu^{3+}$ *ion*

application of the rare-earth complexes in light-emission diodes, it is very important that the color of the emitted light strongly depends on the $Eu^{3+}$ ions concentration in the studied compounds. For the $Eu^{3+}$-doped samples generally used in applications as red phosphors, the color points $x$ and $y$ have to satisfy the following conditions: $x > 0.65$ and $y < 0.35$. In the case of the samples under investigation, the fully concentrated powder sample, *i.e.*, $ZnEu_4W_3O_{16}$, shows a very pure red emission ($x = 0.66$, $y = 0.33$). With decreasing concentration of the active ion $Eu^{3+}$, the color is shifted, and for the 1% $Eu^{3+}$ sample, we obtain white emitters.

**Conclusions.** – A well-emitting material of the formula $ZnEu_4W_3O_{16}$ was formed in a reaction taking place in the solid state between the rare-earth metal tungstate $Eu_2WO_6$ and $ZnWO_4$ mixed in the molar ratio 2:1. X-Ray powder diffraction analysis of the sample obtained by heating the $ZnWO_4/Eu_2WO_6$ mixture showed the presence of one solid phase. The $ZnEu_4W_3O_{16}$ compound crystallizes in the orthorhombic system and is not isostructural with already known $CdRE_4Mo_3O_{16}$ compounds. Photoluminescence studies were carried out for the fully concentrated $ZnEu_4W_3O_{16}$ and yttrium-diluted samples. The dependence of the luminescence properties on the concentration of the active $Eu^{3+}$ ion was established. Intense red emission was obtained on excitation at 394 nm by means of the sharp $^7F_0 \rightarrow {}^5L_6$ line of the $Eu^{3+}$ ion. For diluted samples, the emission from higher $^5D_J$ states of the $Eu^{3+}$ ion was also observed. In these samples, the red emission of $Eu^{3+}$ was also obtained on excitation in the CT band, which indicates an efficient energy transfer from the tungstate group to the $Eu^{3+}$ ion. In these emission spectra, one can observe the broad CT band and narrow lines corresponding to the f-f transition of the $Eu^{3+}$ ion. The analysis of the relative intensities of the $^7F_J$ levels in the emission spectra indicate a low symmetry of the coordination environment. However, the number of sites occupied by the active $Eu^{3+}$ ion in the samples under investigation is not specified yet. Our investigations require supplementary measurements by means of site-selective spectroscopy.

The presented spectroscopic investigations were worthwhile to be developed with the aim to enhance the application of these tungstates to visible-light-emitting phosphors. All the studied samples show a broad CT band and red emission. Selected compositions on this type of phases are suitable in potential applications as red phosphors for white-light generation by means of blue/near-UV-light-emitting diodes (LEDs). The new phosphors may be applied as red-emitting phosphors for white-light-emitting diodes.

## REFERENCES


[1] C. A. Kodaira, H. F. Brito, M. C. F. C. Felinto, *J. Solid State Chem.* **2003**, *171*, 401; C. A. Kodaira, H. F. Brito, O. L. Malta, O. A. Serra, *J. Lumin.* **2003**, *101*, 11.

[2] V. Nagirnyi, E. Feldbach, L. Jonsson, M. Kirm, A. Kotlov, A. Lushchik, V. A. Nefedov, B. I. Zadneprovski, *Nucl. Instrum. Methods Phys. Res., Sect. A* **2002**, *486*, 395.

[3] A. A. Annenkov, M. V. Korzhik, P. Lecoq, *Nucl. Instrum. Methods Phys. Res., Sect. A* **2002**, *490*, 30.

[4] A. M. Srivastava, H. A. Comanzo (to *GE Global Research*), US Patent 6501 100, 2002.

[5] G. Blasse, A. Bril, *J. Chem. Phys.* **1966**, *45*, 2350.

[6] H. J. Borchardt, *J. Chem. Phys.* **1963**, *39*, 504.

[7] A. A. Kaminskii, 'Laser Crystals. Their Physics and Properties', Springer, Berlin – Heidelberg – New York, 1981.

[8] L. Macalik, *Pol. J. Chem.* **1995**, *69*, 286.

[9] J. Hanuza, L. Macalik, B. Macalik, *Acta Phys. Pol., A* **1993**, *84*, 895; J. Hanuza, L. Macalik, B. Macalik, *Acta Phys. Pol., A* **1993**, *84*, 899.

[10] L. Macalik, B. Macalik, W. Strek, J. Legendziewicz, *Eur. J. Solid Inorg. Chem.* **1996**, *33*, 397; L. Macalik, J. Hanuza, J. Sokolnicki, J. Legendziewicz, *Spectrochim. Acta, Part A* **1999**, *55*, 251; L. Macalik, J. Hanuza, J. Legendziewicz, *Acta Phys. Pol., A* **1993**, *84*, 909.

[11] Q. Dai, H. Song, X. Bai, G. Pan, S. Lu, T. Wang, X. Ren, H. Zhao, *J. Phys. Chem. C* **2007**, *11*, 7586.

[12] F. S. Wen, X. Zhao, H. Huo, J.-S. Chen, E. Shu-Lin, J. H. Zhang, *Mater. Lett.* **2002**, *55*, 152.

[13] E. Tomaszewicz, *Solid State Sci.* **2006**, *8*, 508.

[14] D. Taupin, *J. Appl. Crystallogr.* **1968**, *1*, 178; D. Taupin, *J. Appl. Crystallogr.* **1973**, *6*, 380.

[15] D. Louër, M. Louër, *J. Appl. Crystallogr.* **1972**, *5*, 271; A. Boultif, D. Louër, *J. Appl. Crystallogr.* **1991**, *24*, 987.

[16] J. B. Boudet, R. Chevalier, J. P. Fournier, R. Kohlmuller, J. Omaly, *Acta Crystallogr., Sect. B* **1982**, *38*, 2371.

[17] E. Tomaszewicz, *Thermochim. Acta* **2006**, *447*, 69.

[18] V. I. Tsaryuk, V. F. Zolin, *Spectrochim. Acta, Part A* **2001**, *57*, 355.

[19] W. H. Fonger, C. W. Struck, *J. Chem. Phys.* **1970**, *52*, 6364.

[20] G. Blasse, B. C. Grabmaier, 'Luminescence Materials', Springer-Verlag, Heidelberg, 1994.

[21] D. B. Judd, G. Wyszecki, 'Color in Business, Science and Industry', Wiley, New York, 1962, Chap. 2.

[22] R. Shionoya, W. M. Yen, 'Phosphor Handbook, Phosphor Research Society', SRC Press, 1998, p. 459.


*Received April 30, 2009*